MATERIALS SCIENCE

10.1126/sciadv.1500606

Memristive phase switching in two-dimensional 1T-TaS_2 crystals

Masaro Yoshida,[1]* Ryuji Suzuki,[1] Yijin Zhang,[1] Masaki Nakano,[1] Yoshihiro Iwasa[1,2]

Scaling down materials to an atomic-layer level produces rich physical and chemical properties as exemplified in various two-dimensional (2D) crystals including graphene, transition metal dichalcogenides, and black phosphorus. This is caused by the dramatic modification of electronic band structures. In such reduced dimensions, the electron correlation effects are also expected to be significantly changed from bulk systems. However, there are few attempts to realize novel phenomena in correlated 2D crystals. We report memristive phase switching in nano-thick crystals of 1T-type tantalum disulfide (1T-TaS_2), a first-order phase transition system. The ordering kinetics of the phase transition were found to become extremely slow as the thickness is reduced, resulting in an emergence of metastable states. Furthermore, we realized unprecedented memristive switching to multistep nonvolatile states by applying an in-plane electric field. The reduction of thickness is essential to achieve such nonvolatile electrical switching behavior. The thinning-induced slow kinetics possibly make the various metastable states robust and consequently realize the nonvolatile memory operation. The present result indicates that a 2D crystal with correlated electrons is a novel nano-system to explore and functionalize multiple metastable states that are inaccessible in its bulk form.

INTRODUCTION

The memristors are switchable resistors with multiple nonvolatile memory functions (*1*, *2*). Such devices are predicted to play key roles in developing neuromorphic circuits, ultradense information storage, and other applications. One of the promising routes to realizing memristive responses is to use materials with first-order phase transitions, sometimes called phase-change materials (*3*, *4*), providing us with an opportunity to electrically control resistive states. As for the candidate materials for memristors, oxides have been major targets for about 50 years (*5*, *6*). However, the potential of the larger class of nonoxides should also be examined. Because all the memristors have been realized in nanoscale devices (*7*–*9*), two-dimensional (2D) crystals (*10*–*16*) with first-order phase transitions are highly promising. We chose tantalum disulfide with 1T polytype (1T-TaS_2), which is a well-known layered system with first-order charge density wave (CDW) phase transitions (*17*–*21*).

1T-TaS_2 (Fig. 1A), a correlated transition metal dichalcogenide, undergoes successive first-order phase transitions on cooling; one is from an incommensurate CDW (ICCDW) to a nearly commensurate CDW (NCCDW) phase at 350 K, and the other is from an NCCDW to a commensurate CDW (CCDW) phase at 180 K (*17*). In the CCDW phase, 13 Ta atoms form a David-star cluster as shown in Fig. 1A, where the Mott state is simultaneously developed (*18*). The neighboring NCCDW phase is a hexagonal array of CCDW domains (*19*). Only upon warming between 220 and 282 K does there appear another NCCDW phase, consisting of striped triclinic CCDW domains (*19*). In both NCCDW phases, the electronic conduction derives from the mobile carriers in domain boundaries or the discommensuration regions. The schematic pictures of the three CCDW, NCCDW, and ICCDW phases are illustrated in Fig. 1B.

The uniqueness of the nano-thick crystal of 1T-TaS_2 is its unexpected thickness dependence on the CDW phase transition (*22*). As shown in Fig. 1C, the NCCDW-CCDW transition, which is observed in thicker crystals, is completely absent in the 24-nm-thick crystal, whereas the ICCDW-NCCDW transition remains down to the 7-nm-thick crystal. Figure 1D is the summarized electronic phase diagram on cooling at 1 K/min as a function of thickness, showing an abrupt suppression of the NCCDW-CCDW transition and the stabilization of the supercooled NCCDW state in crystals thinner than 40 nm. Another group also reported that the NCCDW-CCDW transition vanishes suddenly with reducing thickness (*23*). In terms of statistical mechanics, a continuous change of a physical parameter such as thickness cannot result in such a sudden disappearance of long-range ordering. We therefore need to use another viewpoint—that of kinetics (*24*)—to understand and functionalize this peculiar first-order phase transition in the nano-system.

RESULTS

Thickness-dependent ordering kinetics in 1T-TaS_2

To clarify the kinetics of the first-order phase transition in 1T-TaS_2 nano-thick crystals, we investigated the cooling rate dependence in many crystals with different thicknesses. Figure 2A displays the temperature (T) dependence of resistivity (ρ) with different cooling/warming rates for the 51-nm-thick crystal. Upon cooling at 5 K/min, the NCCDW-CCDW phase transition was completely suppressed and the supercooled NCCDW state was stabilized down to the lowest temperature. In marked contrast, the 15-nm-thick crystal did not exhibit the NCCDW-CCDW phase transition and the supercooled NCCDW state was stabilized even with the slow cooling rate of 0.3 K/min as shown in Fig. 2B, which reflects its slower kinetics. The systematic cooling rate dependence was observed at low temperatures in the inset of Fig. 2B, where the more rapid the cooling rate is, the lower is the resistivity. Because the equilibrium CCDW state has the highest resistivity, this deviation indicates that the nano-system goes further away from its equilibrium state to metastable states upon rapid cooling.

Taking the kinetics into account, we obtained a more generalized phase diagram as shown in Fig. 2C, displaying the distinct shift of the

[1]Quantum-Phase Electronics Center and Department of Applied Physics, University of Tokyo, Tokyo 113-8656, Japan. [2]RIKEN Center for Emergent Matter Science, Wako 351-0198, Japan.
*Corresponding author. E-mail: masaro-yoshida@mp.t.u-tokyo.ac.jp

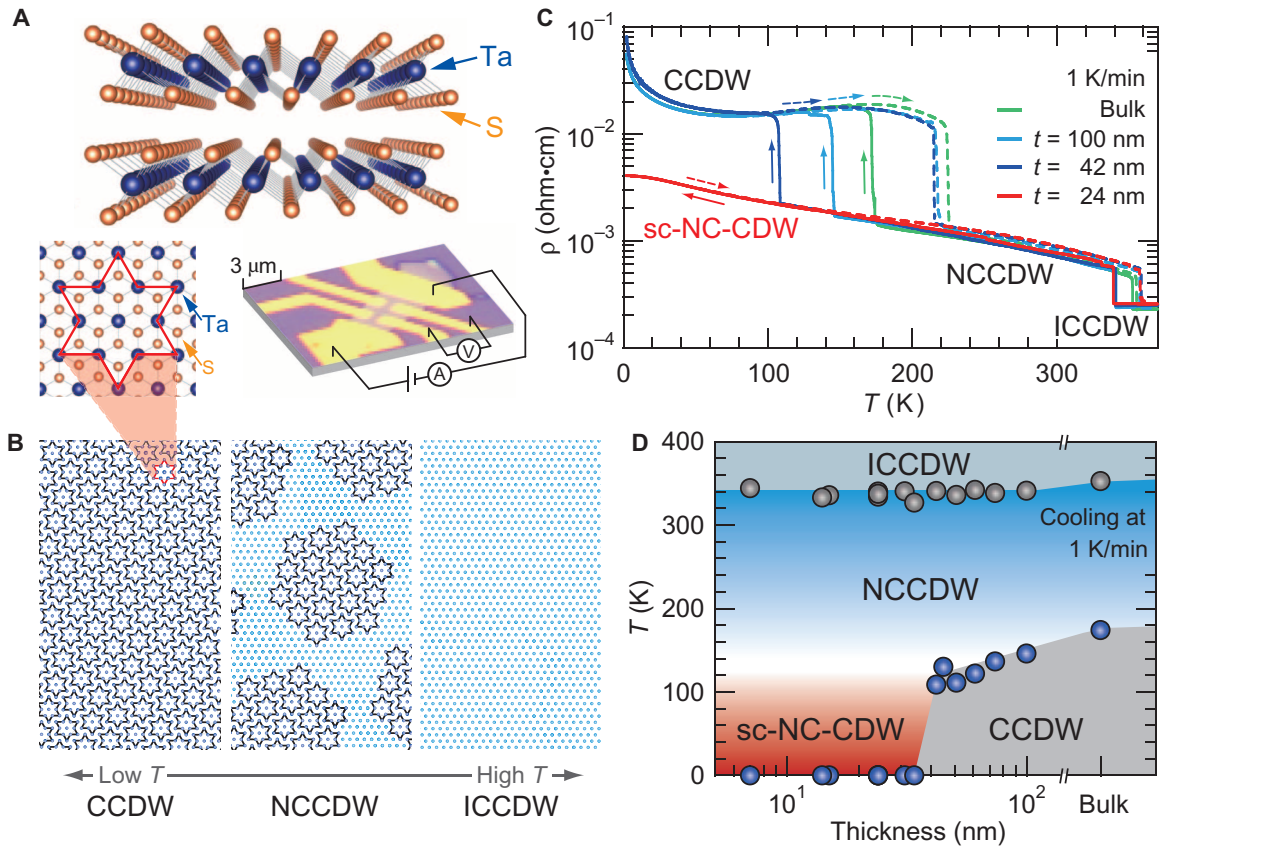

Fig. 1. 1T-TaS_2 single crystals with reduced thickness. (**A**) Crystal structure of the layered 1T-TaS_2, where the planes of tantalum (Ta) atoms are surrounded by sulfur (S) atoms in an octahedral arrangement. The top view of the crystal structure shows a David-star cluster, where 12 Ta atoms within the layer move toward a 13th central Ta atom. Also shown is the optical microscope image of a typical nano-thick crystal device. (**B**) Schematic pictures of a Ta atom network in the CCDW (left), hexagonal NCCDW (middle), and ICCDW (right) phases. The dark blue circles represent the Ta atoms displaced from their undistorted lattice coordinates, forming the David-star clusters. (**C**) Temperature (*T*) dependence of the resistivity (ρ) for bulk and nano-thick crystals of 1T-TaS_2. The solid and broken lines represent the ρ in the cooling and warming cycle, respectively. The notation sc-NCCDW represents supercooled NCCDW. (**D**) Temperature-thickness phase diagram of 1T-TaS_2 nano-thick crystals upon cooling at 1 K/min.

critical thickness for the occurrence of the NCCDW-CCDW transition as a function of cooling rate. This phase diagram enables us to deduce the critical cooling rate (R_c), above which the transition is kinetically avoided upon cooling. Figure 2D is the ground-state phase diagram of 1T-TaS_2 on the thickness-cooling rate plane. The R_c shows a positive correlation with thickness. Here, we can compare the kinetics of the 1T-TaS_2 nano-thick crystals with other materials. For instance, a simple extrapolation indicates that the R_c of a 10-nm-thick crystal should be about 10^{-2} K/min or less, which is as slow as that of an archetypal good glass former, silicon dioxide (SiO_2) (*24*). It is surprising that such a considerable slowdown of kinetics can be realized just by thinning. Discrete systematic variations in the kinetics were recently reported in organic conductors by substituting ions (*25*). The 1T-TaS_2 nano-thick crystal has higher controllability because we can continuously tune the ordering kinetics of the phase transition by changing thickness.

Nonvolatile phase switching in 1T-TaS_2 nano-thick crystals

Such ordering kinetics underlie the nonvolatile switching in phase-change materials between a quenched glassy state and an equilibrium crystalline state by annealing and quenching (*3*, *4*), giving us an opportunity to control the first-order phase transition electrically. We applied in-plane voltage on a 24-nm-thick crystal with a length of 4.8 μm in the supercooled NCCDW state at 95 K and realized a switching operation. Blue curves in Fig. 3 (A and B) are the voltage dependence of current and sheet resistance (R_s), where the current started to decrease gradually above 3 V, followed by the stabilization of a low-current state. Consequently, we observed the appearance of an insulating behavior of the CCDW phase upon cooling, which is shown as a blue curve in Fig. 3C. This voltage-driven transformation can be a "RESET" process, where the local temperature is increased by the Joule heating owing to the current flow, and the crystallization, or growth of CCDW domains, proceeds. Here, the local temperature might not exceed the CCDW-NCCDW transition temperature.

Nonvolatile switching to a metastable state in 1T-TaS_2 nano-thick crystals

Inverse switching, the so-called "SET" process, was also achieved. We applied voltage at 165 K on the crystal in the CCDW phase. As shown in the red curves in Fig. 3 (A and B), current suddenly jumped at 3 V and a high-current state was stabilized. On the basis of the operation mechanism of phase-change memory, this jump of current and R_s may also result from Joule heating, which increases the local temperature

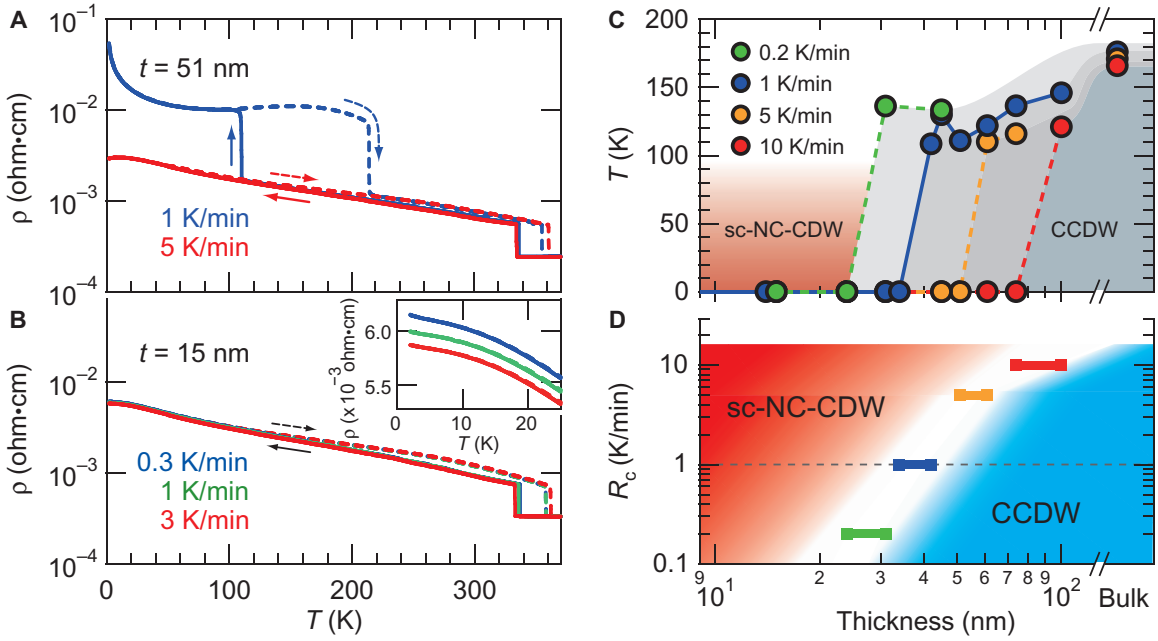

Fig. 2. Cooling rate–dependent behavior of 1T-TaS_2 nano-thick crystals. (**A** and **B**) Temperature (*T*) dependence of the resistivity (ρ) for different temperature-sweeping rates in crystals with thicknesses of 51 nm (A) and 15 nm (B). The inset in (B) is the magnified view of the ρ-*T* curves at low temperatures. (**C**) Temperature-thickness phase diagram of 1T-TaS_2 nano-thick crystals for different temperature-sweeping rates. (**D**) Critical cooling rate (R_c) versus thickness phase diagram.

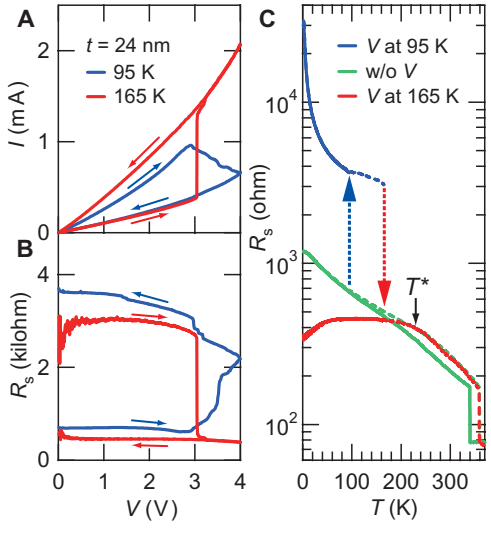

Fig. 3. Voltage-driven phase switching in a 1T-TaS_2 nano-thick crystal. (**A** and **B**) Current-voltage (*I*-*V*) characteristics (A) and simultaneously measured R_s versus voltage curves (B) of a 24-nm-thick crystal measured at 95 K (blue lines) and 165 K (red lines). The sweeping rate was 10 mV/s at 95 K and 50 mV/s at 165 K, respectively. (**C**) Temperature dependence of R_s before and after the applications of in-plane voltage. The green curve was taken before the application of voltage. After applying voltage at 95 K, the crystal was cooled down to 2 K and warmed up to 165 K, which is shown as a blue curve. Subsequently, we applied voltage on the crystal at 165 K and cooled and heated the crystal, which is shown as a red curve. *T** is the temperature above which the crystal recovers to its normal NCCDW phase.

above the CCDW-NCCDW transition temperature in contrast to the RESET process. However, the consequent low-resistivity state was no longer identical to the initial NCCDW state. As shown in Fig. 3C, R_s at 165 K after the application of voltage (red curve) was lower than that of the initial NCCDW state (green curve). Moreover, the R_s-*T* curve never followed the initial curve upon cooling and a metallic conduction was realized below 100 K. The metallic ground state was so robust that it persisted for at least 12 hours at 2 K. Because the conventional phase-change memory is a switching device between two states consisting of low-temperature crystalline and high-temperature glassy phases, our observation of the voltage-induced nonvolatile third state implies that the 1T-TaS_2 nano-thick crystal is not a simple phase-change material. We may, therefore, need to consider another mechanism besides Joule heating to understand the nonvolatile switching behavior.

On the warming-up scan, the R_s-*T* curve finally coincided with the initial curve at a certain temperature *T** = 230 K, and the system had completely recovered to the initial ICCDW phase. The deviation between the green and red R_s-*T* curves in Fig. 3C is qualitatively similar to what was observed upon the rapid cooling shown in Fig. 2, implying that the voltage-induced metallic state (red curves in Fig. 3C) can also be a metastable NCCDW state. Metallic conduction is realized in pressurized or doped 1T-TaS_2 systems (*20*, *23*), but the existence of such a "metastable" metallic state has never been reported in any 1T-TaS_2 system. Here, it was revealed that the application of in-plane voltage is an effective way to induce and stabilize a thermally inaccessible novel nonequilibrium state in 1T-TaS_2 nano-thick crystals.

Memristive phase switching in 1T-TaS_2 nano-thick crystals

The application of voltage under various conditions revealed the memristive nature of 1T-TaS_2 nano-thick crystals. Figure 4A is the voltage dependence of R_s in another 24-nm-thick crystal measured at

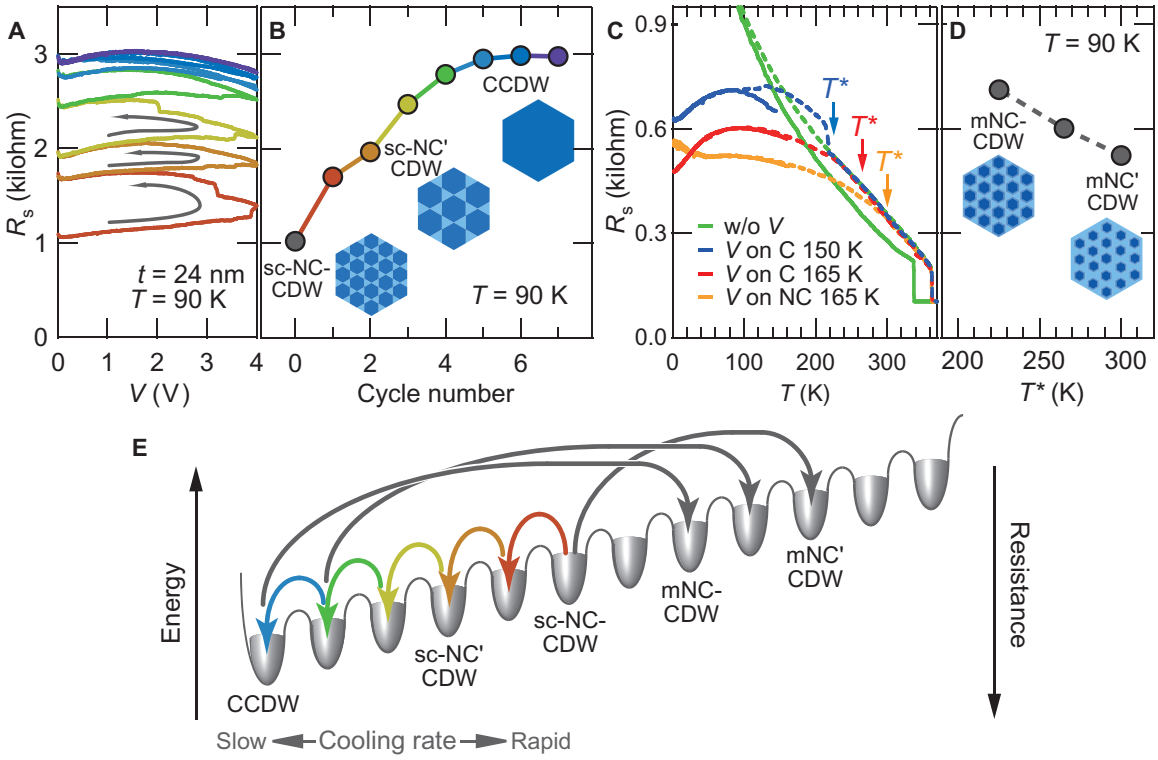

Fig. 4. Memristive characteristics in a 1T-TaS_2 nano-thick crystal. (**A**) R_s versus voltage (V) curves of another 24-nm-thick crystal measured at 90 K with a scanning rate of 10 mV/s. (**B**) Variation of R_s near $V = 0$ V at 90 K as a function of the number of cycles. The applications of voltage realized the switching from a supercooled NCCDW (sc-NCCDW) state through another supercooled NCCDW (sc-NC'CDW) state to the CCDW state. Insets are the possible microscopic structures of each state. The dark blue hexagons refer to CCDW domains composed of David-star clusters, and the light blue areas represent the discommensurations. (**C**) The R_s-T relations before and after the applications of voltage. The green curve was taken before applying voltage. First, the crystal was switched from the supercooled NCCDW state to the CCDW state by applying voltage at 90 K [shown in (A)] and heated to 150 K. The blue curve is the result of cooling and warming measurements after the application of voltage on the crystal in the CCDW phase at 150 K. The red curve is the result of applying voltage on the crystal in the CCDW phase at 165 K. The orange curve was measured after the voltage application on the crystal in the NCCDW phase at 165 K. (**D**) Variation of R_s near $V = 0$ V at 90 K as a function of T^*, above which the system recovers to its normal NCCDW state. Insets are the possible patterns of each metastable state. The notation mNCCDW represents metallic NCCDW. A metallic NCCDW state with a higher T^* (represented by the notation mNC′CDW) may contain a larger area of discommensurations. (**E**) Schematic energy diagram of a 1T-TaS_2 nano-thick memristive system, showing a multiminimum potential. Rainbow- and gray-colored arrows indicate the application of voltage at low and high temperatures, respectively.

90 K, where the crystal was initially in a supercooled NCCDW state. R_s slightly increased and a relatively insulating state was stabilized after a forward and backward voltage scan. Repeated voltage scans resulted in the gradual increase of R_s, followed by saturation to the equilibrium CCDW state after five cycles. We emphasize that the R_s values near $V = 0$ V and the corresponding R_s-V curve did not change as long as the applied voltage was limited to less than 2 V, indicating that the final state after each cycle is nonvolatile and is tuned by the number of cycles. As summarized in Fig. 4B, R_s depends on the history of the voltage application, demonstrating that the system acts as a "resistor with memory" or memristor (*1*, *2*, *5*–*9*, *16*). Because most of the memristors use the tunnel junction configuration of oxide thin films and heterostructures (*5*, *6*, *8*, *9*), the memristive behavior in a lateral structure (*7*, *16*) based on a correlated 2D crystal is unique. By analogy to the semiconducting NCCDW state in the pressurized 1T-TaS_2 (*26*), the increase of R_s may microscopically correspond to the growth of CCDW domains, which is schematically depicted in the insets of Fig. 4B.

The multiple resistive behavior, that is, the memristive characteristic, was also found by applying voltage at higher temperatures. We first cooled down the 24-nm-thick crystal to 90 K and switched from the supercooled state to the CCDW state by the application of voltage as shown in Fig. 4A. Sequentially, we warmed up to 150 K, applied voltage on the crystal in the CCDW state, and obtained conducting R_s-T relations (blue curve in Fig. 4C). In the same way, we observed metallic behavior by applying voltage on the crystal in the CCDW state at 165 K (red curve in Fig. 4C). Moreover, we found that such a conducting state could also be induced by the application of voltage not on the CCDW but on the NCCDW state at 165 K (orange curve in Fig. 4C). In all three conditions, we could observe the recovery to the normal NCCDW state (green curves) upon warming above T^*, indicating that all the low-temperature states are metastable NCCDW states. Figure 4D shows the relation between T^* and the R_s at 90 K deduced from Fig. 4C, showing that T^* increases as the R_s at 90 K decreases. Because the thermodynamically stable CCDW state shows high resistivity, higher T^* is another sign that the system is further away from its thermal equilibrium state.

DISCUSSION

Figure 4E is a schematic energy diagram with multiple CDW states that can be realized in a 1T-TaS_2 nano-thick crystal, where the CCDW domains shrink and the resistance decreases as the system is set further from its equilibrium CCDW state. This diagram presents the potential of the 1T-TaS_2 memristor, where we can possibly tune the area of domains and switch to the various intermediate resistance states by applying in-plane voltages. Recent theoretical and experimental research on light-induced metastable states in 1T-TaS_2 (*21*, *27*) may also give some insight into the microscopic nature of the voltage-induced metastable CDW states.

It should be stressed that the metallic NCCDW states (shown in Fig. 4C) have never been reached by rapid cooling but are accessible only by the application of voltage. Also, the voltage application has a peculiar trend: the application of voltage at low temperatures (indicated by rainbow-colored arrows in Fig. 4E) results in switching toward the equilibrium CCDW state, whereas applying an electric field at higher temperatures (represented by gray arrows in Fig. 4E) always leads the system into metallic NCCDW states. Such highly controllable but nontrivial responses not only raise fundamental questions on the phase-change memories and memristors in nanoscale but also offer potential applications of 2D crystals.

Here, we discuss the mechanism of memristive nonvolatile memory operation, especially of the SET operation in 1T-TaS_2 nano-thick crystals. First, we address the depinning of CDW, which has been intensively investigated in quasi-1D CDW systems: The application of an electric field above the threshold voltage (V_{th}) drives the CDW out of the pinned configuration and consequently realizes switching to a nonlinear conduction state (*28*, *29*). Such a nonlinear conduction is also reported in 1T-TaS_2 bulk single crystals (*30*). However, the 1T-TaS_2 bulk crystal and the nano-thick crystal in the present work are different in V_{th}. In the nano-thick crystal, we observed that V_{th} was about 3 V (see Fig. 3A), corresponding to 6 kV/cm. On the other hand, the V_{th} for bulk single crystals is below 10 V/cm (*30*), which is three orders of magnitude lower than that observed in this work. A more important difference between the nano-thick and bulk crystals is in the volatility of the switched state: The final high-current state was kept after the release of the voltage in the nano-thick crystals, whereas in bulk crystals, the nonlinear conduction vanishes after reducing the voltage. On the basis of these differences in V_{th} and nonvolatility, we conclude that the observed switching behavior in 1T-TaS_2 nano-thick crystals cannot be attributed to the depinning of CDW.

Recently, a carrier-driven collapse of the Mott gap upon applying voltage is proposed for the mechanism to realize phase switching in 1T-TaS_2 (*31*). However, the voltage-induced high-current state is reported to be a volatile ICCDW phase. Also, recently, an asymmetrical charge injection realized by an application of pulsed current is suggested to explain the phase switching in 1T-TaS_2 (*32*), but the switching to a conducting state is reported not to occur if the duration time of voltage exceeds 1 s. This is a marked difference from the memory operation that we observed in the present study. Existing scenarios do not explain the nonvolatile switching behavior observed in the present work, indicating that an exotic switching mechanism is working in 1T-TaS_2 nano-thick crystals.

The present results highlight the robustness of the novel metastable states in 1T-TaS_2 nano-thick crystals induced by an in-plane electric field: Whereas 1T-TaS_2 bulk single crystals show volatile memory operations (*30*), we observed nonvolatile switching behavior in 1T-TaS_2 nano-thick crystals. The sharp contrast between the bulk and nano-thick 1T-TaS_2 systems may be in the speed of the ordering kinetics. As clarified in the cooling rate versus thickness phase diagram (Fig. 2D), the 1T-TaS_2 nano-thick crystals with reduced thickness exhibit extremely slow kinetics. We applied in-plane voltage on nano-thick crystals that are thin enough to realize supercooled NCCDW states at a normal cooling rate of 1 K/min. Therefore, nonequilibrium states are easily stabilized in the nano-system, and the voltage-induced metastable metallic states can be so robust that nonvolatile memory operation is observed. The current results indicate that the thinning-induced slow kinetics possibly plays a crucial role in stabilizing the metastable states, that is, the nonvolatile memory operation.

In conclusion, we demonstrated that the kinetics of the first-order phase transitions in 1T-TaS_2 nano-thick crystals can be systematically controlled by changing the thickness, and we discovered novel metastable metallic states by applying in-plane voltage. The various robust metastable metallic states, which have never been accessed or stabilized in bulk single crystals, are possibly the consequence of the extremely slow kinetics realized by reducing the thickness of the crystal to nanometers. Furthermore, we found a memristive function to switch between multistep nonvolatile metastable states. Our findings present a paradigm that exotic phenomena are hidden not only in 2D crystals with unconventional electronic band structures but also in correlated 2D crystals.

MATERIALS AND METHODS

Device preparations

The 1T-TaS_2 mother single crystal was grown using the conventional chemical vapor transport method with 2% excess sulfur. Nano-thick crystals were isolated from the bulk single crystal by mechanical exfoliation with Scotch tape and transferred onto a doped silicon wafer covered with a layer of thermally grown silicon dioxide. The typical size of cleaved nano-thick crystals was 10 × 10 μm^2. Metal contacts were made through an electron beam lithography process, followed by the sequential deposition of titanium (5 nm) and gold (100 nm). The thickness of the nano-thick crystals was determined by atomic force microscopy.

Measurements

All the transport measurements were performed in Physical Property Measurement System (Quantum Design Inc.) under He-purged conditions. In the cooling rate effect measurement, when we cooled down and warmed up with a sweeping rate of 1 K/min or smaller, we maintained the rate in the whole temperature scan. When we measured with a sweeping rate larger than 1 K/min, we cooled down to T = 50 K with the rapid rate, waited at T = 50 K until the sample temperature was stabilized to T = 50 K, cooled down and warmed up between T = 50 K and T = 2 K at 1 K/min, and warmed up with the rapid rate.

REFERENCES AND NOTES

1. J. J. Yang, D. B. Strukov, D. R. Stewart, Memristive devices for computing. *Nat. Nanotechnol.* **8**, 13–24 (2013).
2. S. D. Ha, S. Ramanathan, Adaptive oxide electronics: A review. *J. Appl. Phys.* **110**, 071101 (2011).

3. M. Wuttig, N. Yamada, Phase-change materials for rewriteable data storage. *Nat. Mater.* **6**, 824–832 (2007).
4. H. Oike, F. Kagawa, N. Ogawa, A. Ueda, H. Mori, M. Kawasaki, Y. Tokura, Phase-change memory function of correlated electrons in organic conductors. *Phys. Rev. B* **91**, 041101(R) (2015).
5. D. B. Strukov, G. S. Snider, D. R. Stewart, R. S. Williams, The missing memristor found. *Nature* **453**, 80–83 (2008).
6. J. J. Yang, M. D. Pickett, X. Li, D. A. A. Ohlberg, D. R. Stewart, R. S. Williams, Memristive switching mechanism for metal/oxide/metal nanodevices. *Nat. Nanotechnol.* **3**, 429–433 (2008).
7. T. Driscoll, H.-T. Kim, B.-G. Chae, M. Di Ventra, D. N. Basov, Phase-transition driven memristive system. *Appl. Phys. Lett.* **95**, 043503 (2009).
8. A. Chanthbouala, V. Garcia, R. O. Cherifi, K. Bouzehouane, S. Fusil, X. Moya, S. Xavier, H. Yamada, C. Deranlot, N. D. Mathur, M. Bibes, A. Barthélémy, J. Grollier, A ferroelectric memristor. *Nat. Mater.* **11**, 860–864 (2012).
9. A. A. Bessonov, M. N. Kirikova, D. I. Petukhov, M. Allen, T. Ryhänen, M. J. A. Bailey, Layered memristive and memcapacitive switches for printable electronics. *Nat. Mater.* **14**, 199–204 (2015).
10. A. K. Geim, K. S. Novoselov, The rise of graphene. *Nat. Mater.* **6**, 183–191 (2007).
11. Q. H. Wang, K. Kalantar-Zadeh, A. Kis, J. N. Coleman, M. S. Strano, Electronics and optoelectronics of two-dimensional transition metal dichalcogenides. *Nat. Nanotechnol.* **7**, 699–712 (2012).
12. M. Chhowalla, H. S. Shin, G. Eda, L.-J. Li, K. P. Loh, H. Zhang, The chemistry of two-dimensional layered transition metal dichalcogenide nanosheets. *Nat. Chem.* **5**, 263–275 (2013).
13. X. Xu, W. Yao, D. Xiao, T. F. Heinz, Spin and pseudospins in layered transition metal dichalcogenides. *Nat. Phys.* **10**, 343–350 (2014).
14. L. Li, Y. Yu, G. J. Ye, Q. Ge, X. Ou, H. Wu, D. Feng, X. H. Chen, Y. Zhang, Black phosphorus field-effect transistors. *Nat. Nanotechnol.* **9**, 372–377 (2014).
15. H. Liu, A. T. Neal, Z. Zhu, Z. Luo, X. Xu, D. Tománek, P. D. Ye, Phosphorene: An unexplored 2D semiconductor with a high hole mobility. *ACS Nano* **8**, 4033–4041 (2014).
16. V. K. Sangwan, D. Jariwala, I. S. Kim, K.-S. Chen, T. J. Marks, L. J. Lauhon, M. C. Hersam, Gate-tunable memristive phenomena mediated by grain boundaries in single-layer MoS_2. *Nat. Nanotechnol.* **10**, 403–406 (2015).
17. J. A. Wilson, F. J. Di Salvo, S. Mahajan, Charge-density waves and superlattices in the metallic layered transition metal dichalcogenides. *Adv. Phys.* **24**, 117–201 (1975).
18. P. Fazekas, E. Tosatti, Charge carrier localization in pure and doped 1T-TaS_2. *Physica* **99B**, 183–187 (1980).
19. R. E. Thomson, B. Burk, A. Zettl, J. Clarke, Scanning tunneling microscopy of the charge-density-wave structure in 1*T*-TaS_2. *Phys. Rev. B. Condens. Matter* **49**, 16899–16916 (1994).
20. B. Sipos, A. F. Kusmartseva, A. Akrap, H. Berger, L. Forró, E. Tutiš, From Mott state to superconductivity in 1T-TaS_2. *Nat. Mater.* **7**, 960–965 (2008).
21. L. Stojchevska, I. Vaskivskyi, T. Mertelj, P. Kusar, D. Svetin, S. Brazovski, D. Mihailovic, Ultrafast switching to a stable hidden quantum state in an electronic crystal. *Science* **344**, 177–180 (2014).
22. M. Yoshida, Y. Zhang, J. Ye, R. Suzuki, Y. Imai, S. Kimura, A. Fujiwara, Y. Iwasa, Controlling charge-density-wave states in nano-thick crystals of 1T-TaS_2. *Sci. Rep.* **4**, 7302 (2014).
23. Y. Yu, F. Yang, X. F. Lu, Y. J. Yan, Y.-H. Cho, L. Ma, X. Niu, S. Kim, Y.-W. Son, D. Feng, S. Li, S.-W. Cheong, X. H. Chen, Y. Zhang, Gate-tunable phase transitions in thin flakes of 1T-TaS_2. *Nat. Nanotechnol.* **10**, 270–276 (2015).
24. D. R. Uhlmann, A kinetic treatment of glass formation. *J. Non-Cryst. Solids* **7**, 337–348 (1972).
25. T. Sato, F. Kagawa, K. Kobayashi, A. Ueda, H. Mori, K. Miyagawa, K. Kanoda, R. Kumai, Y. Murakami, Y. Tokura, Systematic variations in the charge-glass-forming ability of geometrically frustrated θ-$(BEDT\text{-}TTF)_2X$ organic conductors. *J. Phys. Soc. Jpn.* **83**, 083602 (2014).
26. T. Ritschel, J. Trinckauf, G. Garbarino, M. Hanfland, M. v. Zimmermann, H. Berger, B. Büchner, J. Geck, Pressure dependence of the charge density wave in 1*T*-TaS_2 and its relation to superconductivity. *Phys. Rev. B* **87**, 125135 (2013).
27. T. Ritschel, J. Trinckauf, K. Koepernik, B. Büchner, M. v. Zimmermann, H. Berger, Y. I. Joe, P. Abbamonte, J. Geck, Orbital textures and charge density waves in transition metal dichalcogenides. *Nat. Phys.* **11**, 328–331 (2015).
28. J. C. Gill, Thermally initiated phase-slip in the motion and relaxation of charge-density waves in niobium triselenide. *J. Phys. C: Solid State Phys.* **19**, 6589–6604 (1986).
29. G. Grüner, The dynamics of charge-density waves. *Rev. Mod. Phys.* **60**, 1129–1181 (1988).
30. S. Uchida, K. Tanabe, S. Tanaka, Nonlinear conduction in two-dimensional CDW system: 1T-TaS_2. *Solid State Commun.* **27**, 637–640 (1978).
31. M. J. Hollander, Y. Liu, W.-J. Lu, L.-J. Li, Y.-P. Sun, J. A. Robinson, S. Datta, Electrically driven reversible insulator-metal phase transition in 1T-TaS_2. *Nano Lett.* **15**, 1861–1866 (2015).
32. I. Vaskivskyi, I. A. Mihailovic, S. Brazovskii, J. Gospodaric, T. Mertelj, D. Svetin, P. Sutar, D. Mihailovic, Fast non-thermal switching between macroscopic charge-ordered quantum states induced by charge injection. arXiv:1409.3794 (2014).

Acknowledgments: We are grateful to F. Kagawa for fruitful discussions and thankful to J. T. Ye and T. Iizuka for experimental support. **Funding:** This work was supported by Grants-in-Aid for Scientific Research (grant nos. 25000003 and 25708040) from the Japan Society for the Promotion of Science (JSPS). Y.I. was supported by the Strategic International Collaborative Research Program (SICORP-LEMSUPER) of the Japan Science and Technology Agency. M.N. was partly supported by Grant for Basic Science Research Projects from the Sumitomo Foundation. M.Y., R.S., and Y.J.Z. were supported by JSPS through a research fellowship for young scientists. R.S. was supported by the Leading Graduate Program of Materials Education for future leaders in Research, Industry and Technology (MERIT). Y.J.Z was supported by the Advanced Leading Graduate Course for Photon Science (ALPS). **Author contributions:** M.Y. and Y.J.Z. fabricated the devices, and M.Y. performed measurements and analyzed the data. R.S. grew the single crystal. M.Y., M.N., and Y.I. planned and supervised the study. M.Y. and Y.I. wrote the manuscript. **Competing interests:** The authors declare that they have no competing interests. **Data and materials availability:** All the data for this study are available in the manuscript.

Submitted 15 May 2015
Accepted 24 June 2015
Published 2 October 2015
10.1126/sciadv.1500606

Citation: M. Yoshida, R. Suzuki, Y. Zhang, M. Nakano, Y. Iwasa, Memristive phase switching in two-dimensional 1T-TaS_2 crystals. *Sci. Adv.* **1**, e1500606 (2015).